JOURNAL OF SYNCHROTRON RADIATION

ISSN 1600-5775

X-ray radiation damage to biological macromolecules: further insights

Elspeth F. Garman[a]* and Martin Weik[b]*

[a]Laboratory of Molecular Biophysics, Department of Biochemistry, University of Oxford, South Parks Road, Oxford OX1 3QU, UK, and [b]Institut de Biologie Structurale, Univ. Grenoble Alpes, CEA, CNRS, F-38044 Grenoble, France. *Correspondence e-mail: elspeth.garman@bioch.ox.ac.uk, weik@ibs.fr

Keywords: X-ray radiation damage; macromolecular crystallography; SAXS; dose; imaging; scavengers.

Despite significant progress made over more than 15 years of research, structural biologists are still grappling with the issue of radiation damage suffered by macromolecular crystals which is induced by the resultant radiation chemistry occurring during X-ray diffraction experiments. Further insights into these effects and the possible mitigation strategies for use in both diffraction and SAXS experiments are given in eight papers in this volume. In particular, damage during experimental phasing is addressed, scavengers for SAXS experiments are investigated, microcrystals are imaged, data collection strategies are optimized, specific damage to tyrosine residues is reexamined, and room temperature conformational heterogeneity as a function of dose is explored. The brief summary below puts these papers into perspective relative to other ongoing radiation damage research on macromolecules.

There have been concerted efforts over the last 15 years to understand the manifestations and origins of radiation damage suffered by protein crystals during macromolecular crystallography (MX) experiments, and to establish mitigation strategies using various approaches. These have gradually resulted in a deeper understanding of the physical, chemical and structural factors affecting damage rates, and there is a growing literature which seeks to elucidate the pertinent parameters (see for example the special issues of the *Journal of Synchrotron Radiation* arising from talks and posters given at the 2nd to 8th International Workshops on Radiation Damage to Biological Crystalline Samples, published in 2002, 2005, 2007, 2009, 2011, 2013 and 2015, respectively). As the range and scope of the investigations have broadened, so has our appreciation of the complexities of radiation damage phenomena, although a full knowledge of all the processes involved has not yet been achieved. However, the need for this has become more pressing, with the advent of X-ray free-electron lasers (XFEL) and new fourth-generation synchrotron sources such as MAX IV in Lund and NSLS II at Brookhaven now coming on-line with even higher flux densities than hitherto utilized. The high rate of damage inflicted by these X-ray beams has brought the issue of radiation damage during structural biology experiments into even sharper focus. Thus an awareness of the effects of radiation damage both on diffraction and small-angle X-ray scattering (SAXS) data, and on the macromolecular structures derived from them, will become increasingly important.

There are eight papers on various aspects of radiation damage in this special issue of the *Journal of Synchrotron Radiation*. The studies reported here on MX and SAXS experiments were presented at the 9th International Workshop on Radiation Damage to Biological Crystalline Samples held at MAX IV in Lund in March 2016. They include: a reexamination of structural damage to tyrosine residues; two papers on finding the optimum MX data collection strategy for phasing of structures, one using sulfur SAD data in the presence of damage and the other on anomalous phasing with mercury by serial synchrotron data collection; a comparison of helical and standard rotation methods from a radiation damage standpoint; two papers examining damage rates in SAXS experiments and scavengers that can be used to reduce these rates; an analysis of the conformational heterogeneity of side chains as a function of dose in room-temperature

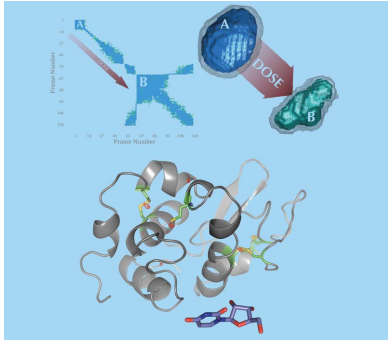

and cryo-crystallography, and, finally, an imaging study on the effects of X-ray irradiation on microcrystals.

X-ray irradiation at cryo-temperatures produces both global and specific radiation damage to crystalline biological macromolecules. The former manifests itself in reciprocal space as a gradual fading of Bragg spot intensities, visually apparent with weak high resolution reflections vanishing first (Gonzalez & Nave, 1994). Other effects that manifest themselves in the processed data with increasing absorbed dose include increasing unit-cell parameters, crystal mosaicity and Wilson *B*-factors, decreasing $I/\sigma(I)$ and a worsening of merging *R*-factors (Burmeister, 2000; Teng & Moffat, 2000; Ravelli & McSweeney, 2000). Specific damage in crystalline proteins appears as changes in electron density maps that originate mainly from disulfide bond breakage or elongation and decarboxylation of acidic amino acid residues (Weik *et al.*, 2000; Ravelli & McSweeney, 2000; Burmeister, 2000; Weik *et al.*, 2002). Compared with proteins, both DNA and RNA are much more robust in terms of specific structural damage as recently shown in systematic studies on DNA-protein (Bury *et al.*, 2015) and RNA-protein complexes (Bury *et al.*, 2016). Protein chromophores are particularly radiation-sensitive as illustrated for example by the recently reported X-ray induced deprotonation of the bilin chromophore in a phytochrome (Li *et al.*, 2015). Specific radiation damage can also be put to good use as shown recently by the collection of a series of 45 consecutive 100 K data sets, where metal-centre reduction by X-ray generated solvated electrons initiated structural changes that allowed elucidation of enzyme catalysis mechanisms in copper nitrite reductase (Horrell *et al.*, 2016).

One of the first reports on specific damage also described loss of electron density on a tyrosine hydroxyl group in the active site of crystalline myrosinase (Burmeister, 2000). Subsequently, this loss has been referred to in the literature as OH loss originating from rupture of the C—O bond, despite cleavage of the phenolic C—O bond never having been reported in the field of tyrosine radiation chemistry. A paper in this issue (Bury *et al.*, 2017) now revisits the initial finding of Tyr –OH group damage in myrosinase. Clear electron density loss of the Tyr –OH group is observed at increasing X-ray doses, consistent with the original report (Burmeister, 2000). Its origin, however, is now identified as being full Tyr aromatic ring displacement and not OH-group cleavage. Bury *et al.*, using an objective new metric called $D_{\rm loss}$, further investigated a range of protein crystal damage series deposited in the Protein Data Bank, establishing that Tyr –OH electron density loss is generally not a dominant damage feature at 100 K, consistent with the high energetic barrier for Tyr phenolic C—O bond scission.

Radiation damage is particularly harmful in single- or multiple-wavelength anomalous dispersion phasing (SAD/MAD) experiments because of the high primary X-ray absorption of anomalous scatterers used for phasing, and because of non-isomorphism generated for instance by changes in unit-cell parameters (Rice *et al.*, 2000; González *et al.*, 2005; Ravelli *et al.*, 2005; Oliéric *et al.*, 2007). Specific secondary radiation damage to sulfur atoms further limits successful phasing in sulfur-SAD experiments. In the latter, the expected anomalous signal is particularly weak, so that low-dose high-multiplicity data should be collected (Olieric *et al.*, 2016). At some point during data collection, however, adding increasingly damage-affected data will cause the deterioration of the quality of the resulting substructure. Storm *et al.* in this issue (Storm *et al.*, 2017) establish a metric that allows identification of the dose limit above which the gain in data quality from increased multiplicity is balanced by radiation-induced deterioration of that data quality. Specifically, a characteristic change in the width of the distribution of anomalous differences as a function of absorbed dose ($\sigma\{\Delta F\}_{\rm D}$) is shown to correlate with the correctness of the resulting sulfur substructure, and is thus suggested as a determinant of the dose corresponding to the *point of diminishing returns*. For cryo-data collection on thaumatin crystals, this dose limit is about 3 MGy (Storm *et al.*, 2017), *i.e.* an order of magnitude lower than the general dose limit (30 MGy; Owen *et al.*, 2006) above which biological information extracted from cryo-MX data is very likely to be compromised by radiation damage. $\sigma\{\Delta F\}_{\rm D}$ is a purely experimental metric that shows great promise for identifying the optimal subset of data in a SAD phasing experiment. Another report in this issue focuses on optimum data collection strategies for SAD phasing at cryo-temperature (Hasegawa *et al.*, 2017). In particular, Hg-SAD phasing of the luciferin regenerating enzyme has been performed using serial synchrotron rotation crystallography (SS-ROX) during which the crystal-containing loop was translated while being rotated. Considerations are described that allow the determination of the optimum helical rotation step depending on various factors such as the multiplicity and the partiality of reflections. Despite the appearance of specific damage at the Hg site above an absorbed dose of 1 MGy, the authors provide evidence for a rise in the anomalous signal up to a dose of 3 MGy because of increasing signal-to-noise ratio, in line with the limit for S-SAD phasing determined with the $\sigma\{\Delta F\}_{\rm D}$ metric by Storm *et al.* (2017).

Defining the optimum data collection strategies for MX has long been a topic of research, and efforts to minimize radiation damage by 'spreading the dose' have been pursued by various means such as helical scanning (rotation + translation during each image; Flot *et al.*, 2010), line scanning (Song *et al.*, 2007) or rotation axis offset (Zeldin, Brockhauser *et al.*, 2013). In this issue, Polsinelli *et al.* (2017) compare standard rotation data collection with the helical strategy on long crystals of three different proteins (human transthyretin with and without brominated ligands, human matrix metalloproteinase and selenomethionine-substituted maltose operon periplasmic protein) using a microbeam [FWHM 10 µm (H) × 5 µm (V)]. Different translations were tested. They conclude that the helical scanning indeed gave an improvement, with one crystal giving better resolution and another giving a more sustained anomalous signal allowing easier phasing. They also suggest that, for bromophenyl moieties bound in proteins, loss of bromine with dose can be a useful metric to monitor damage progression.

Another mitigation strategy that has been extensively tested is the addition of radical scavengers to crystal buffer solutions prior to cryo-cooling or room-temperature (RT) data collection [for a summary of all MX scavenger studies up to 2011 see the supporting information of Allan *et al.* (2013)]. In the literature to date, there are conflicting results on the efficacy of the same compounds, and no consensus has yet emerged as to their effectiveness. Tests of uridine, a previously untried scavenger, for synchrotron-based structural biology techniques (MX and SAXS) are reported in this issue (Crosas *et al.*, 2017). At 1 *M* concentration, uridine was found to be effective in increasing the dose-to-half-intensity, $D_{1/2}$, by a factor of 1.7 for RT MX data collection on chicken egg-white lysozyme crystals, but was found to be ineffective at cryo-temperatures (100 K).

Radiation damage can be an impediment in biological SAXS experiments, since, with dose, solution samples tend to aggregate or possibly fragment, thus impacting the scattering and contributing to the envelope extracted from the data. One strategy used to reduce these deleterious effects of radiation damage is to limit the X-ray exposure to any given volume of sample. This can be achieved by attenuation or defocusing of the X-ray beam, oscillating or flowing the sample within its container, and/or reducing the exposure time (Fischetti *et al.*, 2003; Jeffries *et al.*, 2015; Martel *et al.*, 2012; Pernot *et al.*, 2013). For SAXS, cryo-cooling samples down to 100 K has been reported to increase the dose tolerance of samples by at least two orders of magnitude (Meisburger *et al.*, 2013); however, this method is not commonly used due to technical complications and the reduction in signal due to cryo-protectant in the solution. Another method to increase the dose tolerance of the sample is to add compounds such as ethylene glycol, glycerol, sodium ascorbate or sucrose to the SAXS sample (Kuwamoto *et al.*, 2004; Grishaev, 2012). As well as testing uridine as a scavenger for MX, Crosas *et al.* (2017) tested it in SAXS experiments on lysozyme solutions. They found that it prevented radiation induced aggregation and, at 40 m*M* concentration, was as effective as 5% glycerol. The scavenging effect was proportional to the concentration used for tests up to 100 m*M* and to a dose of 3.8 kGy.

Another paper (Brooks-Bartlett *et al.*, 2017) reports tests on eight radioprotectants (glycerol, ethylene glycol, sodium nitrate, sodium ascorbate, sucrose, trehalose, DTT and TEMPO), and found that glycerol was the most effective at 5 and 10 m*M*, but DTT was the most protective at 1 and 2 m*M*. Associated with this work, tools to automate quantitative exploration of radiation damage in SAXS experiments have been developed. These allow convenient visualization and analysis of results from the CorMap method of frame comparison (Franke *et al.*, 2015).

Room-temperature crystallography is notoriously difficult to carry out because of an increase in radiation sensitivity by two orders of magnitude compared with cryo-temperatures (Nave & Garman, 2005; Warkentin & Thorne, 2010), manifested as global radiation damage. Consequently, only a handful of studies have addressed specific radiation damage at RT so far since several data sets are required to follow damage as a function of the absorbed X-ray dose. In a seminal paper, Blake and Phillips observed that the structure factors of some reflections from myoglobin crystals increased, while others decreased, leading them to suggest that specific structural damage to certain amino acids must be occurring (Blake & Philips, 1962), a hypothesis confirmed later for RT crystals (Helliwell, 1988). The occurrence of specific damage at RT remains controversial, however, with some reports showing evidence for disulfide damage (Southworth-Davies *et al.*, 2007; Coquelle *et al.*, 2015), while others do not (Roedig *et al.*, 2016), including Crosas *et al.* in this issue (Crosas *et al.*, 2017). Despite increased radiation sensitivity, RT data collection is desirable because the modification of conformational heterogeneity within the crystalline protein that may occur during cryo-cooling is avoided, potentially providing physiologically more meaningful structures (Fraser *et al.*, 2011). Careful control experiments must be conducted to deconvolute radiation-induced from temperature-induced changes (Keedy *et al.*, 2015). In this issue, Russi *et al.* addressed the question as to whether or not the conformational variation of proteins at RT is dominated by radiation damage (Russi *et al.*, 2017). They monitored the number of alternate side-chain conformations as a function of the absorbed dose in three different crystalline proteins at room- and cryo-temperatures. At both temperatures, the conformational heterogeneity did not depend on the absorbed dose, leading the authors to conclude that increased conformational heterogeneity at room- *versus* cryo-temperatures is observed, despite the presence, and not as a result, of radiation damage. Russi and co-workers also found evidence for specific radiation damage to disulfide bonds at RT, yet to a lesser extent than at 100 K. The description and understanding of global and specific radiation damage at RT will greatly benefit from the recent development of serial synchrotron crystallography (Gati *et al.*, 2014), where the dose is spread over a large number of crystals that are presented to the X-ray beam within a capillary (Stellato *et al.*, 2014), by microfluidic means (Heymann *et al.*, 2014), on solid supports or by viscous jets (Nogly *et al.*, 2015; Botha *et al.*, 2015).

Serial synchrotron crystallography data collection techniques generally employ microcrystals. Their usefulness has increased markedly since the advent of beamlines at synchrotrons which can deliver microbeams (<10 µm) that are intense enough to allow measurable diffraction from very small crystal volumes. This raises the question of whether radiation damage rates and effects are the same for micro-crystals as they are for bigger crystals. Over ten years ago Nave & Hill (2005) pointed out that the photoelectrons produced when X-rays are absorbed by microcrystals would be able to escape the surface and thus would not lose all their energy in the sample. Hence the absorbed dose would be reduced and, since damage is proportional to dose at cryo-temperatures, it might be expected that damage rates would be lower for smaller crystals. However, until now this effect had not yet been experimentally validated. Incidentally, the program *RADDOSE-3D* (Zeldin, Gerstel *et al.*, 2013) used to estimate doses in MX does not yet take into account possible photoelectron escape. *RADDOSE-3D* assumes instead that

the total energy carried by the photoelectrons is absorbed within the sample, thus overestimating the dose in such small samples. This deficiency could usefully be rectified in the near future. A paper in this issue (Coughlan *et al.*, 2017) describes reciprocal-space mapping and Bragg coherent diffractive imaging experiments on six cryo-cooled microcrystals (<2 μm, characterized using transmission electron microscopy) of chicken egg-white lysozyme using micrometre-sized beams. Single reflections between 13 and 17 Å resolution were monitored as a function of dose, and the more traditional metrics of intensity-loss, rocking curve width and lattice expansion (in terms of relative *d*-spacing) plotted. Additionally, two metrics only obtainable from the coherent measurements were investigated: the volumes of the reciprocal-space map and real-space images as they varied with increasing dose, obtained from performing 3D Fourier transforms on the phased data to give 3D images of the crystals. The results show that the diffracting volume shrinks with increasing radiation damage and also suggest that surface areas of the crystals are damaged more quickly than the inner parts, although confirmation of this will be required by further characterization. In addition, the data lead the authors to suggest that they have evidence for smaller crystals having a longer lifetime than would be predicted for macroscopic ones, as predicted by Nave & Hill (2005).

Serial crystallography at XFELs, so-called serial femtosecond crystallography [SFX (Chapman *et al.*, 2011; Boutet *et al.*, 2012)], allows collection of crystallographic data before specific chemical and structural damage has had the time to develop within the crystalline macromolecule, so-called 'diffraction-before-destruction' (Neutze *et al.*, 2000). In most cases, the resulting structures are indeed devoid of specific damage (Hirata *et al.*, 2014; Chreifi *et al.*, 2016). At the very high doses absorbed when deliberately using unattenuated long (>50 fs) XFEL pulses, however, global (Lomb *et al.*, 2011; Barty *et al.*, 2012) and specific (Lomb *et al.*, 2011; Nass *et al.*, 2015; Galli *et al.*, 2015) radiation damage can occur. Further insight into the progression of specific damage on the ultrafast time scale is expected to emerge from SFX experiments in the near future.

Acknowledgements

We thank Ian Carmichael and Edward Snell for their critical reading of this manuscript. The 9th International Workshop on Radiation Damage to Crystalline Biological Samples, at which most of the work in this special issue was presented, would not have been possible without the invaluable support of MAX IV who hosted it, and the hard work of the Local Organizing Committee of Thomas Ursby and Marjolein Thunnissen. We are most grateful to them, and also for financial support from our co-organisers, the COST Action CM1306 'Movement and Mechanism in Molecular Machines'.

References

Allan, E. G., Kander, M. C., Carmichael, I. & Garman, E. F. (2013). *J. Synchrotron Rad.* **20**, 23–36.

Barty, A., Caleman, C., Aquila, A., Timneanu, N., Lomb, L., White, T. A., Andreasson, J., Arnlund, D., Bajt, S., Barends, T. R. M., Barthelmess, M., Bogan, M. J., Bostedt, C., Bozek, J. D., Coffee, R., Coppola, N., Davidsson, J., DePonte, D. P., Doak, R. B., Ekeberg, T., Elser, V., Epp, S. W., Erk, B., Fleckenstein, H., Foucar, L., Fromme, P., Graafsma, H., Gumprecht, L., Hajdu, J., Hampton, C. Y., Hartmann, R., Hartmann, A., Hauser, G., Hirsemann, H., Holl, P., Hunter, M. S., Johansson, L., Kassemeyer, S., Kimmel, N., Kirian, R. A., Liang, M. N., Maia, F., Malmerberg, E., Marchesini, S., Martin, A. V., Nass, K., Neutze, R., Reich, C., Rolles, D., Rudek, B., Rudenko, A., Scott, H., Schlichting, I., Schulz, J., Seibert, M. M., Shoeman, R. L., Sierra, R. G., Soltau, H., Spence, J. C. H., Stellato, F., Stern, S., Struder, L., Ullrich, J., Wang, X., Weidenspointner, G., Weierstall, U., Wunderer, C. B. & Chapman, H. N. (2012). *Nat. Photon.* **6**, 35–40.

Blake, C. C. F. & Philips, D. C. (1962). *Vienna: Int. At. Energ. Agency.* pp. 183–191.

Botha, S., Nass, K., Barends, T. R. M., Kabsch, W., Latz, B., Dworkowski, F., Foucar, L., Panepucci, E., Wang, M., Shoeman, R. L., Schlichting, I. & Doak, R. B. (2015). *Acta Cryst.* D**71**, 387–397.

Boutet, S., Lomb, L., Williams, G. J., Barends, T. R., Aquila, A., Doak, R. B., Weierstall, U., DePonte, D. P., Steinbrener, J., Shoeman, R. L., Messerschmidt, M., Barty, A., White, T. A., Kassemeyer, S., Kirian, R. A., Seibert, M. M., Montanez, P. A., Kenney, C., Herbst, R., Hart, P., Pines, J., Haller, G., Gruner, S. M., Philipp, H. T., Tate, M. W., Hromalik, M., Koerner, L. J., van Bakel, N., Morse, J., Ghonsalves, W., Arnlund, D., Bogan, M. J., Caleman, C., Fromme, R., Hampton, C. Y., Hunter, M. S., Johansson, L. C., Katona, G., Kupitz, C., Liang, M., Martin, A. V., Nass, K., Redecke, L., Stellato, F., Timneanu, N., Wang, D., Zatsepin, N. A., Schafer, D., Defever, J., Neutze, R., Fromme, P., Spence, J. C., Chapman, H. N. & Schlichting, I. (2012). *Science*, **337**, 362–364.

Brooks-Bartlett, J. C., Batters, R. A., Bury, C. S., Lowe, E. D., Ginn, H. M., Round, A. & Garman, E. F. (2017). *J. Synchrotron Rad.* **24**, 63–72.

Burmeister, W. P. (2000). *Acta Cryst.* D**56**, 328–341.

Bury, C. S., Carmichael, I. & Garman, E. F. (2017). *J. Synchrotron Rad.* **24**, 7–18.

Bury, C., Garman, E. F., Ginn, H. M., Ravelli, R. B. G., Carmichael, I., Kneale, G. & McGeehan, J. E. (2015). *J. Synchrotron Rad.* **22**, 213–224.

Bury, C. S., McGeehan, J. E., Antson, A. A., Carmichael, I., Gerstel, M., Shevtsov, M. B. & Garman, E. F. (2016). *Acta Cryst.* D**72**, 648–657.

Chapman, H. N., Fromme, P., Barty, A., White, T. A., Kirian, R. A., Aquila, A., Hunter, M. S., Schulz, J., DePonte, D. P., Weierstall, U., Doak, R. B., Maia, F. R., Martin, A. V., Schlichting, I., Lomb, L., Coppola, N., Shoeman, R. L., Epp, S. W., Hartmann, R., Rolles, D., Rudenko, A., Foucar, L., Kimmel, N., Weidenspointner, G., Holl, P., Liang, M., Barthelmess, M., Caleman, C., Boutet, S., Bogan, M. J., Krzywinski, J., Bostedt, C., Bajt, S., Gumprecht, L., Rudek, B., Erk, B., Schmidt, C., Hömke, A., Reich, C., Pietschner, D., Strüder, L., Hauser, G., Gorke, H., Ullrich, J., Herrmann, S., Schaller, G., Schopper, F., Soltau, H., Kühnel, K. U., Messerschmidt, M., Bozek, J. D., Hau-Riege, S. P., Frank, M., Hampton, C. Y., Sierra, R. G., Starodub, D., Williams, G. J., Hajdu, J., Timneanu, N., Seibert, M. M., Andreasson, J., Rocker, A., Jönsson, O., Svenda, M., Stern, S., Nass, K., Andritschke, R., Schröter, C. D., Krasniqi, F., Bott, M., Schmidt, K. E., Wang, X., Grotjohann, I., Holton, J. M., Barends, T. R., Neutze, R., Marchesini, S., Fromme, R., Schorb, S., Rupp, D., Adolph, M., Gorkhover, T., Andersson, I., Hirsemann, H., Potdevin, G., Graafsma, H., Nilsson, B. & Spence, J. C. (2011). *Nature (London)*, **470**, 73–77.

Chreifi, G., Baxter, E. L., Doukov, T., Cohen, A. E., McPhillips, S. E., Song, J., Meharenna, Y. T., Soltis, S. M. & Poulos, T. L. (2016). *Proc. Natl Acad. Sci. USA*, **113**, 1226–1231.
Coquelle, N., Brewster, A. S., Kapp, U., Shilova, A., Weinhausen, B., Burghammer, M. & Colletier, J.-P. (2015). *Acta Cryst.* D**71**, 1184–1196.
Coughlan, H. D., Darmanin, C., Kirkwood, H. J., Phillips, N. W., Hoxley, D., Clark, J. N., Vine, D. J., Hofmann, F., Harder, R. J., Maxey, E. & Abbey, B. (2017). *J. Synchrotron Rad.* **24**, 83–94.
Crosas, E., Castellvi, A., Crespo, I., Fulla, D., Gil-Ortiz, F., Fuertes, G., Kamma-Lorger, C. S., Malfois, M., Aranda, M. A. G. & Juanhuix, J. (2017). *J. Synchrotron Rad.* **24**, 53–62.
Fischetti, R. F., Rodi, D. J., Mirza, A., Irving, T. C., Kondrashkina, E. & Makowski, L. (2003). *J. Synchrotron Rad.* **10**, 398–404.
Flot, D., Mairs, T., Giraud, T., Guijarro, M., Lesourd, M., Rey, V., van Brussel, D., Morawe, C., Borel, C., Hignette, O., Chavanne, J., Nurizzo, D., McSweeney, S. & Mitchell, E. (2010). *J. Synchrotron Rad.* **17**, 107–118.
Franke, D., Jeffries, C. M. & Svergun, D. I. (2015). *Nat. Methods*, **12**, 419–422.
Fraser, J. S., van den Bedem, H., Samelson, A. J., Lang, P. T., Holton, J. M., Echols, N. & Alber, T. (2011). *Proc. Natl Acad. Sci. USA*, **108**, 16247–16252.
Galli, L., Son, S.-K., Klinge, M., Bajt, S., Barty, A., Bean, R., Betzel, C., Beyerlein, K. R., Caleman, C., Doak, R. B., Duszenko, M., Fleckenstein, H., Gati, C., Hunt, B., Kirian, R. A., Liang, M., Nanao, M. H., Nass, K., Oberthür, D., Redecke, L., Shoeman, R., Stellato, F., Yoon, C. H., White, T. A., Yefanov, O., Spence, J. & Chapman, H. N. (2015). *Struct. Dyn.* **2**, 041703.
Gati, C., Bourenkov, G., Klinge, M., Rehders, D., Stellato, F., Oberthür, D., Yefanov, O., Sommer, B. P., Mogk, S., Duszenko, M., Betzel, C., Schneider, T. R., Chapman, H. N. & Redecke, L. (2014). *IUCrJ*, **1**, 87–94.
Gonzalez, A. & Nave, C. (1994). *Acta Cryst.* D**50**, 874–877.
González, A., von Delft, F., Liddington, R. C. & Bakolitsa, C. (2005). *J. Synchrotron Rad.* **12**, 285–291.
Grishaev, A. (2012). *Current Protocols in Protein Science*, Unit 17.14 (doi:10.1002/0471140864.ps1714s70).
Hasegawa, K., Yamashita, K., Murai, T., Nuemket, N., Hirata, K., Ueno, G., Ago, H., Nakatsu, T., Kumasaka, T. & Yamamoto, M. (2017). *J. Synchrotron Rad.* **24**, 29–41.
Helliwell, J. R. (1988). *J. Cryst. Growth*, **90**, 259–272.
Heymann, M., Opthalage, A., Wierman, J. L., Akella, S., Szebenyi, D. M. E., Gruner, S. M. & Fraden, S. (2014). *IUCrJ*, **1**, 349–360.
Hirata, K., Shinzawa-Itoh, K., Yano, N., Takemura, S., Kato, K., Hatanaka, M., Muramoto, K., Kawahara, T., Tsukihara, T., Yamashita, E., Tono, K., Ueno, G., Hikima, T., Murakami, H., Inubushi, Y., Yabashi, M., Ishikawa, T., Yamamoto, M., Ogura, T., Sugimoto, H., Shen, J. R., Yoshikawa, S. & Ago, H. (2014). *Nat. Methods*, **11**, 734–736.
Horrell, S., Antonyuk, S. V., Eady, R. R., Hasnain, S. S., Hough, M. A. & Strange, R. W. (2016). *IUCrJ*, **3**, 271–281.
Jeffries, C. M., Graewert, M. A., Svergun, D. I. & Blanchet, C. E. (2015). *J. Synchrotron Rad.* **22**, 273–279.
Keedy, D. A., Kenner, L. R., Warkentin, M., Woldeyes, R. A., Hopkins, J. B., Thompson, M. C., Brewster, A. S., Van Benschoten, A. H., Baxter, E. L., Uervirojnangkoorn, M., McPhillips, S. E., Song, J., Alonso-Mori, R., Holton, J. M., Weis, W. I., Brunger, A. T., Soltis, S. M., Lemke, H., Gonzalez, A., Sauter, N. K., Cohen, A. E., van den Bedem, H., Thorne, R. E. & Fraser, J. S. (2015). *Elife* **4**, e07574.
Kuwamoto, S., Akiyama, S. & Fujisawa, T. (2004). *J. Synchrotron Rad.* **11**, 462–468.
Li, F., Burgie, E. S., Yu, T., Héroux, A., Schatz, G. C., Vierstra, R. D. & Orville, A. M. (2015). *J. Am. Chem. Soc.* **137**, 2792–2795.
Lomb, L., Barends, T. R., Kassemeyer, S., Aquila, A., Epp, S. W., Erk, B., Foucar, L., Hartmann, R., Rudek, B., Rolles, D., Rudenko, A., Shoeman, R. L., Andreasson, J., Bajt, S., Barthelmess, M., Barty, A., Bogan, M. J., Bostedt, C., Bozek, J. D., Caleman, C., Coffee, R., Coppola, N., DePonte, D. P., Doak, R. B., Ekeberg, T., Fleckenstein, H., Fromme, P., Gebhardt, M., Graafsma, H., Gumprecht, L., Hampton, C. Y., Hartmann, A., Hauser, G., Hirsemann, H., Holl, P., Holton, J. M., Hunter, M. S., Kabsch, W., Kimmel, N., Kirian, R. A., Liang, M., Maia, F. R., Meinhart, A., Marchesini, S., Martin, A. V., Nass, K., Reich, C., Schulz, J., Seibert, M. M., Sierra, R., Soltau, H., Spence, J. C., Steinbrener, J., Stellato, F., Stern, S., Timneanu, N., Wang, X., Weidenspointner, G., Weierstall, U., White, T. A., Wunderer, C., Chapman, H. N., Ullrich, J., Strüder, L. & Schlichting, I. (2011). *Phys. Rev. B*, **84**, 214111.
Martel, A., Liu, P., Weiss, T. M., Niebuhr, M. & Tsuruta, H. (2012). *J. Synchrotron Rad.* **19**, 431–434.
Meisburger, S. P., Warkentin, M., Chen, H., Hopkins, J. B., Gillilan, R. E., Pollack, L. & Thorne, R. E. (2013). *Biophys. J.* **104**, 227–236.
Nass, K., Foucar, L., Barends, T. R. M., Hartmann, E., Botha, S., Shoeman, R. L., Doak, R. B., Alonso-Mori, R., Aquila, A., Bajt, S., Barty, A., Bean, R., Beyerlein, K. R., Bublitz, M., Drachmann, N., Gregersen, J., Jönsson, H. O., Kabsch, W., Kassemeyer, S., Koglin, J. E., Krumrey, M., Mattle, D., Messerschmidt, M., Nissen, P., Reinhard, L., Sitsel, O., Sokaras, D., Williams, G. J., Hau-Riege, S., Timneanu, N., Caleman, C., Chapman, H. N., Boutet, S. & Schlichting, I. (2015). *J. Synchrotron Rad.* **22**, 225–238.
Nave, C. & Garman, E. F. (2005). *J. Synchrotron Rad.* **12**, 257–260.
Nave, C. & Hill, M. A. (2005). *J. Synchrotron Rad.* **12**, 299–303.
Neutze, R., Wouts, R., van der Spoel, D., Weckert, E. & Hajdu, J. (2000). *Nature (London)*, **406**, 752–757.
Nogly, P., James, D., Wang, D., White, T. A., Zatsepin, N., Shilova, A., Nelson, G., Liu, H., Johansson, L., Heymann, M., Jaeger, K., Metz, M., Wickstrand, C., Wu, W., Båth, P., Berntsen, P., Oberthuer, D., Panneels, V., Cherezov, V., Chapman, H., Schertler, G., Neutze, R., Spence, J., Moraes, I., Burghammer, M., Standfuss, J. & Weierstall, U. (2015). *IUCrJ*, **2**, 168–176.
Oliéric, V., Ennifar, E., Meents, A., Fleurant, M., Besnard, C., Pattison, P., Schiltz, M., Schulze-Briese, C. & Dumas, P. (2007). *Acta Cryst.* D**63**, 759–768.
Olieric, V., Weinert, T., Finke, A. D., Anders, C., Li, D., Olieric, N., Borca, C. N., Steinmetz, M. O., Caffrey, M., Jinek, M. & Wang, M. (2016). *Acta Cryst.* D**72**, 421–429.
Owen, R. L., Rudino-Pinera, E. & Garman, E. F. (2006). *Proc. Natl Acad. Sci. USA*, **103**, 4912–4917.
Pernot, P., Round, A., Barrett, R., De Maria Antolinos, A., Gobbo, A., Gordon, E., Huet, J., Kieffer, J., Lentini, M., Mattenet, M., Morawe, C., Mueller-Dieckmann, C., Ohlsson, S., Schmid, W., Surr, J., Theveneau, P., Zerrad, L. & McSweeney, S. (2013). *J. Synchrotron Rad.* **20**, 660–664.
Polsinelli, I., Savko, M., Rouanet-Mehouas, C., Ciccone, L., Nencetti, S., Orlandini, E., Stura, E. A. & Shepard, W. (2017). *J. Synchrotron Rad.* **24**, 42–52.
Ravelli, R. B. & McSweeney, S. M. (2000). *Structure*, **8**, 315–328.
Ravelli, R. B. G., Nanao, M. H., Lovering, A., White, S. & McSweeney, S. (2005). *J. Synchrotron Rad.* **12**, 276–284.
Rice, L. M., Earnest, T. N. & Brunger, A. T. (2000). *Acta Cryst.* D**56**, 1413–1420.
Roedig, P., Duman, R., Sanchez-Weatherby, J., Vartiainen, I., Burkhardt, A., Warmer, M., David, C., Wagner, A. & Meents, A. (2016). *J. Appl. Cryst.* **49**, 968–975.
Russi, S., González, A., Kenner, L. R., Keedy, D. A., Fraser, J. S. & van den Bedem, H. (2017). *J. Synchrotron Rad.* **24**, 73–82.
Song, J., Mathew, D., Jacob, S. A., Corbett, L., Moorhead, P. & Soltis, S. M. (2007). *J. Synchrotron Rad.* **14**, 191–195.
Southworth-Davies, R. J., Medina, M. A., Carmichael, I. & Garman, E. F. (2007). *Structure*, **15**, 1531–1541.
Stellato, F., Oberthür, D., Liang, M., Bean, R., Gati, C., Yefanov, O., Barty, A., Burkhardt, A., Fischer, P., Galli, L., Kirian, R. A., Meyer, J., Panneerselvam, S., Yoon, C. H., Chervinskii, F., Speller, E., White, T. A., Betzel, C., Meents, A. & Chapman, H. N. (2014). *IUCrJ*, **1**, 204–212.

Storm, S. L. S, Dall'Antonia, F., Bourenkov, G. & Schneider, T. R. (2017). *J. Synchrotron Rad.* **24**, 19–28.
Teng, T. & Moffat, K. (2000). *J. Synchrotron Rad.* **7**, 313–317.
Warkentin, M. & Thorne, R. E. (2010). *Acta Cryst.* D**66**, 1092–1100.
Weik, M., Bergès, J., Raves, M. L., Gros, P., McSweeney, S., Silman, I., Sussman, J. L., Houée-Levin, C. & Ravelli, R. B. G. (2002). *J. Synchrotron Rad.* **9**, 342–346.
Weik, M., Ravelli, R. B., Kryger, G., McSweeney, S., Raves, M. L., Harel, M., Gros, P., Silman, I., Kroon, J. & Sussman, J. L. (2000). *Proc. Natl Acad. Sci. USA*, **97**, 623–628.
Zeldin, O. B., Brockhauser, S., Bremridge, J., Holton, J. M. & Garman, E. F. (2013). *Proc. Natl Acad. Sci. USA*, **110**, 20551–20556.
Zeldin, O. B., Gerstel, M. & Garman, E. F. (2013). *J. Appl. Cryst.* **46**, 1225–1230.